

Infrared Signatures and Models of Circumstellar Dust Disks

Kenneth Wood

University of St Andrews

Abstract

This contribution describes theoretical models for the temperature and density structure of circumstellar disks and what properties of disks may be determined from analysis of disk images and spectral energy distributions. I will summarize contributions from several groups that have developed publicly available radiation transfer codes and grids of models of disk spectra. In addition, tools for fitting spectra from large datasets, such as the growing Spitzer archive, are now available.

1 Introduction

The existence of pre-main-sequence circumstellar dust disks was inferred from infrared observations that showed a flux excess above that expected from a stellar photosphere (Mendoza 1968). The infrared excess was interpreted as reprocessing of starlight to longer wavelengths by circumstellar dust. If spherically distributed, the mass of dust required to produce the observed infrared fluxes would extinct the stars at optical wavelengths, therefore equatorial disks were identified as the source of the infrared excess emission. Since these early observations the continual improvement in the size and sensitivity of infrared, sub-mm and mm detectors, and several dedicated infrared space missions (IRAS, ISO, Spitzer) has made research on star formation and disks one of the most active fields in astronomy. As described in this contribution, with each new instrument or mission the observations of disks place more demands on theoreticians and modelers to refine theories of star and planet formation.

Disks are seen as a key ingredient of the star formation process, they provide a channel for accreting material onto the forming star and through disk locking processes can regulate the stellar angular momentum evolution and thus play a crucial role in the distribution of stellar rotation periods in star clusters. The observed infrared excesses from disks are now well modeled as

thermal emission from dust heated by stellar radiation and the dissipation of energy through viscous accretion (see review by Dullemond et al. 2007). The shape of the infrared and mm spectral energy distribution from an individual disk is determined by the disk inclination, size, shape, dust composition, accretion rate, and the stellar temperature and luminosity. Many degeneracies exist when modeling spectral energy distributions, but the large grids of models now available from public radiation transfer codes enable us to analyze data to obtain sensible and realistic limits on disk properties without over-interpretation (Robitaille et al. 2007).

Observations of large numbers of disks in many star forming regions now allows disks to be studied in a range of environments with the goal of determining general properties and timescales of disk evolution. For example, ground based near-infrared observations of many star clusters at the $3.6\mu\text{m}$ L band, indicate that the fraction of sources within a cluster exhibiting infrared excess declines as a function of cluster age, from which it is inferred that the timescale for disk dissipation is around ten million years (Haisch et al. 2001). This timescale has knock on implications for theories of planet formation within disks, implying the planet building phase within disks is typically less than ten million years.

Disks are generally associated with the “Class II” spectral energy distributions from the pre-main-sequence infrared spectral classification scheme originally proposed by Lada (1987). In this scheme Class I spectra are those where direct starlight is extinguished over a wide range of viewing angles of the protostar and the infrared emission is dominated by that from infalling envelopes associated with early stages of star formation. Optical and near-infrared emission in Class I spectra arises from starlight scattered off the walls of cavities in the envelopes carved by jets and outflows. Objects exhibiting Class II spectra have many clear lines of sight to the central star and produce the classic infrared signatures of star plus disk systems. Class III spectra are akin to reddened photospheres and are associated with pre-main-sequence stars with little or no circumstellar material. Examples of spectra from radiation transfer models of the different spectral classes are shown in Figure 1.

Since the original I, II, III classification scheme was adopted, a fourth class has been added. The “Class 0” spectra are extreme examples of Class I spectra and are generally well fit with cool (10 K to 20 K) single temperature blackbodies and are very faint in the optical and near-infrared (e.g., Andre, Ward-Thompson, & Barsony 2000). Taken as a whole, the Class 0, I, II, and III spectra are seen as an evolutionary sequence with Class 0 being the youngest sources embedded in natal material and Class III spectra marking the dissipation of circumstellar material prior to the protostar reaching the main sequence. Obviously, degeneracies may exist where some viewing angles and circumstellar structures result in disks and envelopes producing spectra that span Classes 0 through III (e.g., Robitaille et al. 2006, 2007), but in general

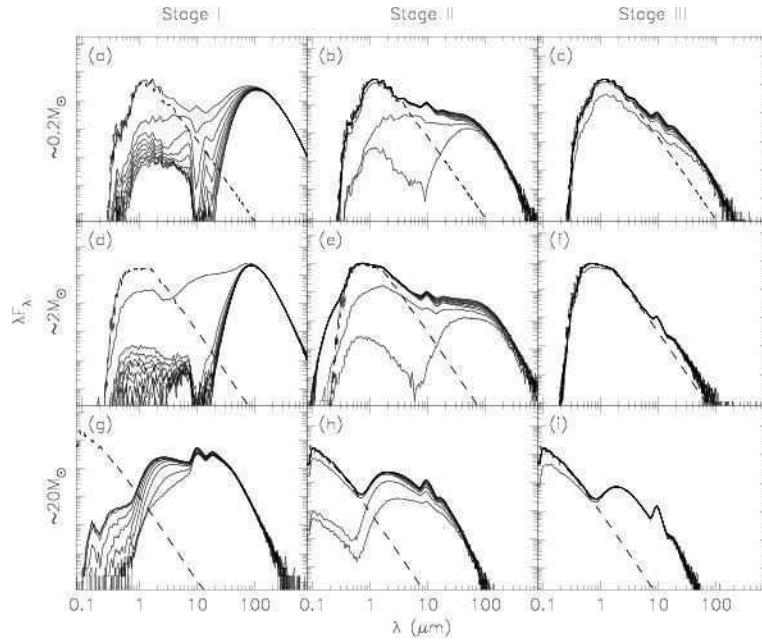


Fig. 1. Model spectra for a range of protostar models spanning embedded infalling envelopes, through low mass disk-only systems. Figure from Robitaille et al. (2006).

the classification scheme reflects an object's evolutionary status.

2 Disk models

Disks are often categorized as passive or active, depending on whether their heating is from accretion (active) or reprocessing of starlight (passive). In reality, both processes must be present in any disk, with the relative heating contributions dependent on the accretion rate through the disk and luminosity of the central protostar. Systems exhibiting FU Orionis outbursts have spectra that are well modeled by active accretion disks, while the observed infrared excesses from Classical T Tauri stars are in general dominated by disks heated by starlight, but with a non-negligible accretion component. The following sections describe radiation transfer models for disks of increasing accuracy and complexity.

2.1 *Semi-analytic models: flat disks*

The first models of spectra from accretion disks were presented by Lynden-Bell & Pringle (1974) who demonstrated that the radial temperature structure of a flat (i.e., infinitely thin) disk accreting at a steady rate \dot{M} , surrounding a

star of mass M and radius R_\star is

$$T(r)^4 = \frac{3GM\dot{M}}{8\pi\sigma r^3} \left[1 - \sqrt{R_\star/r} \right], \quad (1)$$

which for large radii tends to $T(r) \propto r^{-3/4}$ (see also the review by Pringle 1981). Treating the disk as a series of blackbodies, the resulting disk-integrated spectrum for pole-on viewing is readily calculated with a numerical integration between disk inner and outer radii, r_{\min} and r_{\max} ,

$$F_\nu \propto \int_{r_{\min}}^{r_{\max}} B_\nu[T(r)] 2\pi r dr. \quad (2)$$

The $r^{-3/4}$ temperature dependence also arises in passive flat disks which are optically thick to stellar radiation. Adams & Shu (1986) showed that the temperature for a flat disk heated by starlight is given by

$$T(r)^4 = T_\star^4 \left[\sin^{-1}(R_\star/r) - (R_\star/r) \sqrt{1 - (R_\star/r)^2} \right] / \pi \quad (3)$$

which tends to $T(r) \propto r^{-3/4}$ at large radii. In the limit of an infinite disk radius, a flat disk can intercept one quarter of the stellar luminosity, $L_\star/4$. The disk's thermal spectrum may again be calculated by numerically integrating Eq. 2.

2.2 *Semi-analytic models: flared disks*

For many Classical T Tauri stars the infrared excesses are larger than can be explained by flat disk models, implying a radial temperature structure that is less steep than the $r^{-3/4}$ law for active and passive flat disks. A natural way to flatten the disk temperature structure is to invoke disk flaring where the disk scaleheight increases with radius away from the star. Such a scenario is a natural consequence for disks in vertical hydrostatic equilibrium with gas and dust well mixed throughout in which case the density structure is of the form,

$$\rho(r, z) = \rho_0 e^{-\frac{1}{2}[z/h(r)]^2} (r/R_0)^{-\alpha}, \quad (4)$$

where ρ_0 is the density at some fiducial radius R_0 and $h(r)/r = c_s(r)/\Omega(r)$ is the scaleheight of the disk, assuming the disk is vertically isothermal with c_s and Ω being the isothermal sound speed and rotational velocity respectively. If the temperature structure is of the form $T(r) \propto r^{-q}$ then the disk scaleheight has the form $h(r) \propto r^{(3-q)/2}$. The flared disk surface can intercept more than

the $L_*/4$ of a flat disk and this results in a shallower radial temperature gradient and larger infrared excess (Kenyon & Hartmann 1987). In general if the scaleheight has the form $h \sim r^\beta$ then the surface density $\Sigma \sim r^{\beta-\alpha}$. As discussed below, irradiated accretion disks in vertical hydrostatic equilibrium have $\Sigma \sim r^{-1}$ and $T \sim r^{-1/2}$ (D'Alessio et al. 1998), so a good starting point for disk models is to adopt $\alpha = 2.25$, $\beta = 1.25$.

In Kenyon & Hartmann's disk models the surface where stellar photons were intercepted was assumed to lie at a few scaleheights above the disk midplane. In general, stellar photons will be absorbed when they reach the "optical depth one surface" in the upper layers of the disk. The precise location of this surface as a function of radius depends on the disk mass, structure and dust opacity, but is generally found to be around three to five scaleheights above the midplane. It should be noted that at these heights there is very little mass, but the dust opacity is sufficient to absorb starlight so that the "disk photosphere" lies well outside the majority of the disk mass.

2.3 Vertical temperature gradients and inner edges

The semi-analytic models described above assumed disks were vertically isothermal and often optically thick with a gray opacity. The first detailed calculations to explore disk temperature structure and emergent spectra were presented by Calvet et al. (1991) and extended by D'Alessio et al. (1998, 1999, 2001). Their calculations showed that an irradiated accretion disk has a hot surface and cool interior. When disk heating by accretion is included the disk midplane also becomes hot leading to a vertical temperature structure that cools with depth from the irradiated surface, before warming up in the midplane regions where accretion heating dominates (see Fig. 4 in D'Alessio et al. 1998). The warm surface layer is responsible for silicate emission features present in the spectra of many T Tauri disks.

The essential features (hot surface and cool interior) of the calculations by Calvet, D'Alessio, and collaborators are captured in the two-layer disk model of Chiang & Goldreich (1997, 1999). In their model, the surface is heated by direct starlight and attains the optically thin dust temperature. The model assumes that half of the stellar radiation absorbed by the disk is radiated towards and heats the midplane regions. This naturally produces a two temperature disk and reproduces many of the features of disk spectra.

A problem faced by the techniques described above is that although the resulting spectra could explain observations of T Tauri disks, the near-infrared excesses observed in Herbig Ae/Be disks were often under-predicted. Several scenarios were suggested to alleviate the discrepancy between models and data

including very high disk accretion rates (Hillenbrand et al. 1992) and emission from circumstellar envelopes (Hartmann, Kenyon, & Calvet 1993). A more obvious answer was to include emission from the inner edge of a dust disk that is illuminated directly by the star. Since semi-analytic models up until this time only considered stellar radiation entering the disk surface, near-infrared excess emission from the disk inner edge was not accounted for.

In the absence of dynamical disruption to the disk, the inner edge of the dust disk will occur at the dust sublimation temperature, typically around 1600 K. Stellar radiation intercepted and reprocessed at this temperature will therefore dominate the near-infrared, just the wavelength region where previous models had failed. This idea was first incorporated into semi-analytic disk models by Natta et al. (2001) and Dullemond et al. (2001), and subsequently refined by Isella & Natta (2005) and Tannirkulam, Harries, & Monnier (2007) to consider the shape of the disk edge due to different dust species sublimating at different temperatures and pressures.

2.4 Gas in disks

The above discussion has focussed on infrared excess emission arising from circumstellar dust and has not considered the gaseous component. Groups that have made progress in studying the dynamics, radiation transfer and chemistry within disks comprising dust and gas include Kamp & Dullemond (2004), Nomura et al. (2007), D'Alessio et al. (1998). Among the reasons why it is important to study gas in disks is that the gas provides observational signatures of accretion, especially in the hot inner disk regions where temperatures due to stellar heating and accretion are too high for dust to survive. Currently popular models for magnetospheric accretion link the star and inner disk and subsequent stellar angular momentum evolution is sensitive to the location where the inner disk is coupled to the star by accretion streams (see review by Bouvier et al. 2007). As these hot inner regions are likely to be free of dust, it is only through gas signatures that we may determine the location of the inner edge of a magnetospherically truncated disk. These inner disk regions may be probed by several techniques including high resolution spectroscopy, especially CO overtone emission (see review by Najita et al. 2007), and more recently near infrared interferometry (e.g., Akeson et al. 2005). Another technique that may prove fruitful in studying inner gas disks is high resolution spectropolarimetry of optical and near infrared emission and absorption lines (Vink et al. 2005).

2.5 *Monte Carlo radiation transfer*

Many of the approximations in semi-analytic disk models can be relaxed using Monte Carlo radiation transfer techniques. Monte Carlo codes can incorporate multiple, non-isotropic scattering; allow for 3D geometries and illumination; and treat radiation transfer in 2D and 3D so naturally include radial transport of photons within the disk. Reprocessing of stellar radiation at the disk inner edge is also naturally included in disk models that use Monte Carlo radiation transfer techniques.

Recent advances in the development of efficient radiative equilibrium algorithms allow fast and accurate dust radiative equilibrium calculations in 3D (Lucy 1999; Bjorkman & Wood 2001; Indebetouw et al. 2006). With the ever increasing speed and memory of desktop computers previous concerns regarding the speed and convergence of Monte Carlo techniques are no longer relevant. However, Monte Carlo should never be regarded as the cure for all radiation transport problems. The technique is best suited to regions where optical depths are not extremely large and so for very dense regions, alternative radiation transfer methods may be required. For example, the inner regions of some disks may be very dense and in such cases it is more accurate to use Monte Carlo for the upper, optically thin layers and employ a diffusion approximation to determine the temperature and reprocessing of radiation for the densest layers (e.g., Bjorkman, Whitney, & Wood 2002). An alternative that is always available is to kill off Monte Carlo photon packets after they have undergone a fixed number of interactions (scattering, absorption, re-emission events). This results in the codes not conserving energy, but our experience of disk models shows that energy is conserved typically to better than 1%. In such cases the emergent spectrum is accurately predicted, but the temperature in the dense regions is not determined. Clearly for models with very dense regions, a combination of Monte Carlo and diffusion techniques provides the most accurate solution for the temperature structure and emerging spectrum.

2.6 *The structure of irradiated accretion disks*

The disk models described above assume a fixed density structure for which a temperature structure and emergent spectral energy distribution are calculated. Kenyon & Hartmann (1987) assumed disks were optically thick to stellar radiation and that the dust and gas are well mixed and in vertical hydrostatic equilibrium. Disk heating by viscous accretion and starlight and enforcing vertical hydrostatic equilibrium at each radius in the disk then leads to an iterative solution for the disk temperature structure and scaleheight.

The optically thick assumption was relaxed in a series of papers by D’Alessio et al. (1998, 1999, 2001) who calculated disk structure models for irradiated accretion disks. They found for disks with a steady accretion rate throughout and viscosity parameterized by the Shakura & Sunyaev (1973) α parameter the temperature structure and surface density tended to $T(r) \sim r^{-1/2}$ and $\Sigma(r) \sim r^{-1}$. In their models the disk vertical temperature structure displays the same hot surface, cooler interior and hot midplane (due to accretion) shown by Calvet et al (1991).

The models of D’Alessio and collaborators did not include heating of nor any possible shadowing of outer disk regions by the optically thick inner edge of the disk. Models of the structure of passive disks that include inner edge effects were published by Dullemond & Dominik (2004). Their models had different radial dependences for the disk surface density and the accompanying cartoons for the disk structure suggested some situations (in particular disks with very steep surface densities, $\Sigma \sim r^{-4}$) could result in disk structures where the outer disk lies entirely in the shadow of the disk inner edge. It was therefore proposed that these “self shadowed” disks may be responsible for the low infrared excesses seen in the “Type II” Herbig Ae/Be stars (Meeus et al. 2001).

The disk structure cartoons presented by Dullemond & Dominik (2004, Fig. 8) should not be interpreted as the inner edge casting a shadow and leading to a “collapse” of the outer disk. In our disk models where we calculate temperatures using Monte Carlo radiation transfer and then iterate to determine hydrostatic disk structure, we find that the disk inner edge does not have a significant influence on the disk structure, especially for disks with surface densities $\Sigma \sim r^{-1}$ (e.g., Akeson et al. 2005). Also, it is the very steep surface densities adopted in some of the Dullemond & Dominik (2004) models that have the greater influence on the disk spectrum and inner edge effects play a minor role. Indeed, the temperature structure for disks with steep power laws still exhibits the characteristics of a hot surface and cooler interior, as shown in Figure 2. Note also that the r^{-4} disk is less flared than the r^{-1} disk because for steep surface density gradients the mass is concentrated toward smaller radii. Therefore the outer disk is optically thinner and the disk photosphere is at a smaller height above the midplane than for disks with shallower surface density gradients.

Recent models leave the scaleheight of the disk’s inner edge as a free parameter to be fit depending on the level of the near infrared excess observed from a particular disk (e.g., Pontoppidan et al. 2007). It appears that heating by starlight is not sufficient to give inner disk scaleheights required to reproduce observations over a wide range of disk masses surrounding low mass brown dwarfs through higher mass A stars (e.g., Scholz et al. 2006; Pontoppidan et al. 2007). Therefore other effects such as reprocessing of starlight by a disk wind

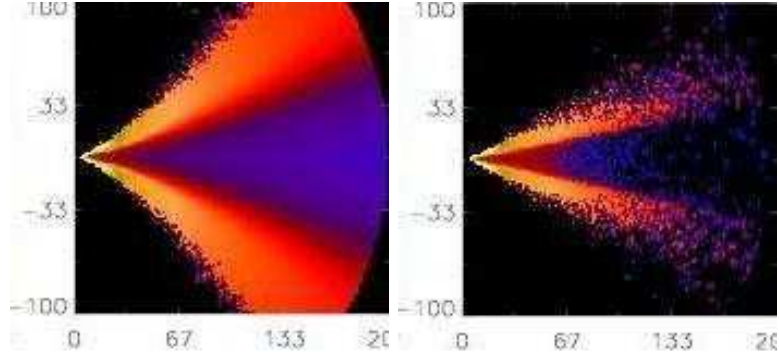


Fig. 2. Two dimensional model temperature structures for passive disks in hydrostatic equilibrium. Both disks have a mass of $0.01M_{\odot}$ and are irradiated by an A0 star. Axes are labeled in AU. Upper panel shows a disk with surface density $\Sigma \propto r^{-1}$ and the disk in lower panel has $\Sigma \propto r^{-4}$. Both disks show the hot upper layers and cool interior characteristic of passive disks.

or some other mechanism is required for increasing the inner disk scaleheight above that expected from stellar heating plus hydrostatic equilibrium.

3 Publicly available radiation transfer codes and grids of models

The following groups have made publicly available radiation transfer codes and grids of spectra for different model disk systems.

3.1 Radiation transfer codes

The semi-analytic disk models described above are straightforward to code and it is very instructive to develop your own versions of the flat, flared, and two-layer disk models. A version of the Chiang & Goldreich model, including reprocessing of starlight at the disk inner edge, is available from Kees Dullemond. His website also contains links to other radiation transfer codes he has developed:

www.mpia-hd.mpg.de/homes/dullemond/radtrans

Monte Carlo radiation transfer codes for calculating dust temperatures, spectra, and multiwavelength images include Sebastian Wolf's code (Wolf 2003) at:

www.mpia-hd.mpg.de/homes/swolf/mc3d-public/mc3d-public.html

and the Monte Carlo radiation transfer codes described by Whitney et al.

(2003):

caravan.astro.wisc.edu/protostars

3.2 *Grids of models*

Grid of irradiated accretion disk models for a range of stellar properties, disk accretion rates, disk radii, and dust properties calculated using techniques described in papers by D'Alessio et al. (1998, 1999, 2001):

www.cfa.harvard.edu/youngstars/dalessio

Grid of protostar models and associated on-line tool for fitting models to data for a wide range of evolutionary states from highly embedded sources through very low mass disks, described in Robitaille et al. (2006, 2007):

caravan.astro.wisc.edu/protostars

4 **Disk properties**

Many degeneracies exist when fitting models to data, however, in general terms different wavelength regimes provide information on different disk properties and sizescales as described below.

4.1 *Near and mid infrared: $1\mu\text{m} - 20\mu\text{m}$*

This wavelength regime provides information on the inner disk out to around 10 AU sizes, and models are sensitive to the size of any inner disk holes, the shape of the inner edge of the disk, and the accretion rate through the disk. In addition this wavelength regime contains spectral features due to silicates and very small grains and polycyclic aromatic hydrocarbon (PAH) molecules which emit from the hot upper disk layers.

One of the first systematic studies of near infrared emission from disks was that of Lada & Adams (1992) who presented data and disk models for Classical T Tauri Stars, Herbig Ae/Be stars and Classical Be stars. Their flat disk models showed that the near infrared emission from T Tauri and Herbig Ae/Be stars could be modeled with flat dust disks with inner hole sizes corresponding to roughly where the dust sublimation temperature would occur.

Classical Be stars have smaller disks with infrared excess emission from free-free emission (e.g., Wood et al. 1997). Subsequent investigations have refined the Lada & Adams (1992) analysis to include the more detailed disk structure models described above. However, the general finding is still that the majority of T Tauri and Herbig Ae/Be disks are well modeled with irradiated accretion disks where the inner edge of the optically thick region coincides with temperatures of around 1600 K, typically associated with dust destruction.

The disk accretion rate influences the near and mid infrared spectrum because accretion is an important heating source for the inner disk regions. In addition, currently popular magnetospheric accretion models have around half of the accretion luminosity liberated on hot spots on the surface of the star, explaining the observed ultraviolet and optical excess emission and photometric variability of Classical T Tauri stars (e.g., Kenyon et al. 1994).

Inner holes and gaps in disks manifest themselves by producing emission deficits in the infrared spectrum. It is very difficult to distinguish from infrared spectra disk gaps from other effects such as the overall disk structure. However, future high resolution images of disks in scattered light (Varniere et al. 2006) and at thermal wavelengths (Wolf et al. 2002) may detect disk gaps. In contrast, the presence of inner holes in the dust disk is much more easily identified by deficits in the near and mid-infrared spectrum. The first disk system to be identified as possessing a large (several AU) inner hole was GM Aur (Koerner, Sargent, & Beckwith 1993). Inner dust holes result in near-infrared deficits with starlight being intercepted and reprocessed to longer wavelengths at the inner edge of the dust disk. The larger the hole, the cooler will be the inner edge and the stellar radiation will be reprocessed at longer wavelengths as illustrated in Figure 3. One of the major advances provided by the Spitzer Space Telescope is to markedly increase the number of such systems known (e.g., Furlan et al. 2007; Espaillat et al. 2007; Calvet et al. 2005).

Note that the Spitzer data is providing information on holes in the *dust* disk and does not probe any optically thin gas that may exist inside the dust. So a disk can have a large inner dust hole, but still exhibit accretion signatures as gas and in some models small dust particles, can accrete through the inner disk regions on to the star. To determine where the physical inner edge of the disk lies requires other observational techniques such as near-infrared interferometry (e.g. Akeson et al. 2005), spectropolarimetry (Vink et al. 2005), or high resolution spectroscopy in search of gas emission from the inner disk (Najita et al. 2007).

The upper layers of disks are optically thin, directly exposed to starlight, are warmer than the interior, and for inclinations where the star is not obscured, produce emission features from silicate grains and possibly also PAH molecules. The $9.7\mu\text{m}$ and $18\mu\text{m}$ silicate features are ubiquitous in the disks of

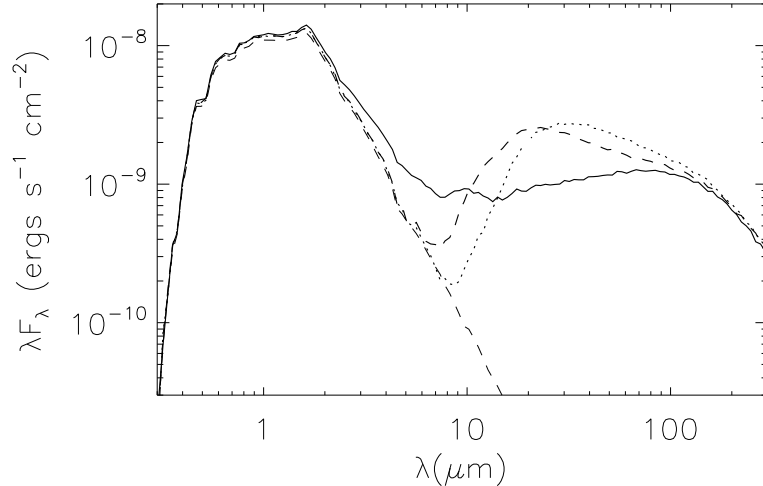


Fig. 3. Effect of inner disk hole sizes on a disk surrounding a T Tauri star. Radiation removed at short wavelengths is reprocessed to longer wavelengths corresponding to temperature of inner edge of the disk. Hole sizes are dust destruction radius (solid line), 1 AU (dashed line), and 10 AU (dotted line).

brown dwarfs to massive stars, while the non-thermal PAH emission depends on the strength of the exciting stellar ultraviolet radiation. PAH features are therefore more readily observed around hotter stars (Habart et al. 2006). The existence of small silicate grains in disk upper layers is expected from models of dust coagulation, segregation, and settling where the larger grains settle more rapidly to the midplane and so have a smaller scaleheight than small grains (e.g., Dullemond & Dominik 2005).

A combination of high resolution infrared spectroscopy from Spitzer and high spatial resolution mid infrared imaging has led to new grain studies. The shape of the features is governed by the grain type, amorphous or crystalline silicate, and the imaging studies indicate that the fraction of crystalline grains is high in the inner regions and this has been incorporated into recent disk models (Dullemond et al. 2007)

4.2 Mid to far infrared: $20\mu\text{m} - 300\mu\text{m}$

The shape of the disk is the main factor determining the flux levels in the mid to far infrared and as such this regime probes the flared structure of disks, whether dust is in vertical hydrostatic equilibrium with gas, and the degree of dust settling from that expected from hydrostatic models.

Kenyon & Hartmann (1987) first showed that flared disks provide more mid to far infrared excess emission than flat disks and that the flux excess levels are sensitive to the dust scaleheight. Miyake & Nakagawa (1995) modeled IRAS data on T Tauri disks showing that disks could be modeled with a range of

geometries from flat to flared disks. Further observations from ISO and Spitzer are now allowing us to study the structure of large numbers of disks in many star forming regions. The picture emerging is similar to that found by Miyake & Nakagawa that some disks exhibit flared structures close to that expected for hydrostatic equilibrium models (REFS), while the infrared emission from other disks indicates the dust is in a flatter distribution being settled and not in vertical hydrostatic equilibrium with the gas (Chiang et al. 2001; D’Alessio et al. 2001; Lada et al. 2006; D’Alessio et al. 2006).

Disk evolution models must therefore be able to explain the observed disk shapes (dust coagulation and settling) along with the opening of gaps and discriminate among models for the clearing of the inner disk. Such models for inside-out disk evolution include: disk-planet interactions, grain filtration, stellar UV irradiation, and magneto-rotational instabilities.

4.3 Far infrared through mm: 300 μ m — 3mm

At these wavelengths the bulk of the disk emission is often optically thin and so the spectral slope directly probes the wavelength dependence of the dust opacity, which in turn provides information on the dust size distribution. Observations at optically thin millimeter wavelengths also provide estimates of the disk dust mass, assuming the dust opacity and disk temperature structure is known. However, the dust opacity is very uncertain and depends on the size and shape of the grain size distribution, so what can safely be estimated from modeling is the product of dust mass and opacity. In general although dust dominates the disk opacity, it makes up only a few percent of the total disk mass and the total disk mass is therefore dependent on the dust to gas ratio. As a result disk masses are very uncertain.

In general if the dust opacity at long wavelengths is of the form $\kappa_\nu \sim \nu^\beta$ then the slope of the spectrum is approximately of the form $\lambda F_\nu \sim \nu^{3+\beta}$ (Beckwith & Sargent 1991). Models of grain size distributions that reproduce the observed interstellar extinction law have a long wavelength opacity $\kappa \sim \lambda^{-2}$, while larger grains have shallower wavelength dependent opacities and hence produce shallower long wavelength spectra. Interstellar dust grain models typically have grain sizes extending up to a few microns (Mathis et al. 1977; Draine & Lee 1984), whereas dust models required to fit observations of disks require the grain size distribution to extend up to meter sizes (Natta et al. 2007).

4.4 *Degeneracies and a couple of cautionary notes*

The previous sections have outlined information that can be gained from modeling data in different wavelength regimes. Degeneracies among models for a particular dataset will exist, especially for systems with limited wavelength coverage. For example, the spectrum is very insensitive to the outer disk radius (Beckwith et al. 1990; Scholz et al. 2006). However, as described below using large grids of models prevents over-interpretation of data and large wavelength coverage enables tighter constraints to be placed on disk properties.

Much of the disk modeling has focussed on systems where the central star is revealed. Modeling spectra of edge-on disks is somewhat more problematic because the central star is not seen so determining its properties must also enter into the modeling and fitting procedures. Two cautionary notes on edge-on disk systems are that the bolometric luminosity is inclination dependent and that the extinction to the central star cannot be determined from the optical and near infrared spectrum. These may seem like obvious statements, but occasionally such errors are made.

For a spherical system the bolometric luminosity may be estimated by integrating the observed spectrum, F_ν , over all frequencies. However, the non-spherical circumstellar geometries associated with all phases of star formation mean that the bolometric luminosity cannot be estimated in this way. Edge-on disk systems are the most extreme example where the optical through mid infrared emission (starlight and reprocessed emission from the inner disk) cannot reach the observer due to the large optical depths, typically in the range of 10^3 to 10^6 . At optical wavelengths, edge-on disks are seen only in scattered light. This means that the usual techniques for determining extinction to the central star cannot be used because no direct starlight is present in the spectrum — e^{-10^6} is a very wee number!

An example of incorrect analysis to determine bolometric luminosity and also extinction is the analysis of observations of the object known as Gomez’s Hamburger (Ruiz et al. 1987). Hubble Space Telescope images show that this object resembles an edge-on disk and based on estimates of its bolometric luminosity REF estimated its distance to be around 3 kpc. However, taking into account the inclination dependence of the spectrum, our models suggest the object is much closer at around 360 pc. Figure 4 shows models for the HST images and spectrum. Our new Monte Carlo radiation transfer models described in Wood et al. (2007, in preparation) incorporate non-equilibrium emission from PAHs and very small grains using opacities and emissivities from Draine & Li (2007). In this model photons that are absorbed by PAH and VSG grains are reprocessed to the infrared by choosing frequencies from the emissivity tables from Draine & Li (2007) that depend on the mean intensity

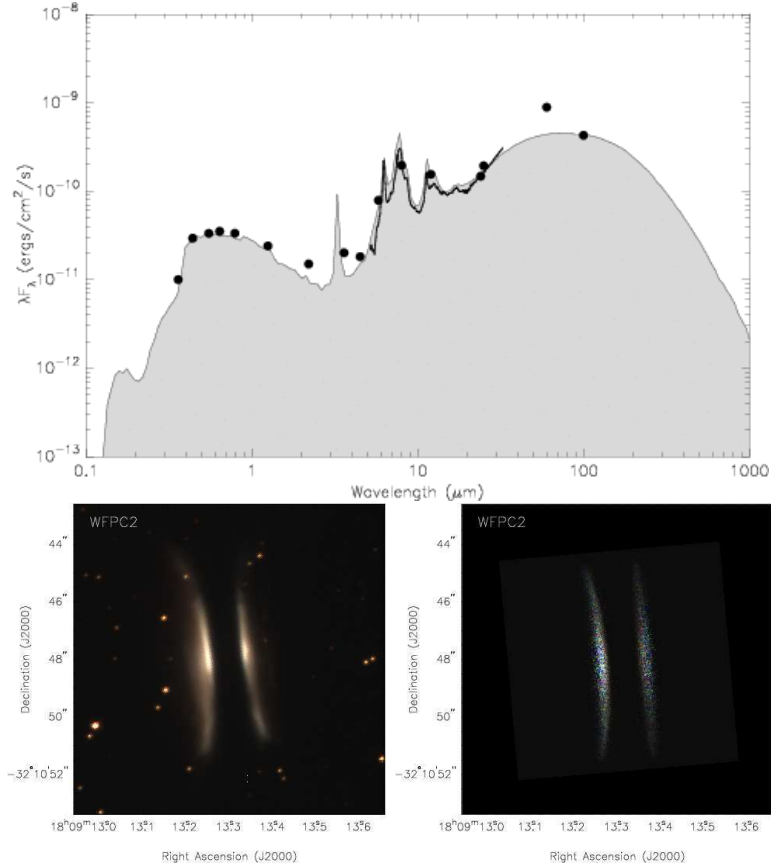


Fig. 4. Upper panel shows a SED model and observed spectra for Gomez’s Hamburger. Note the prominent PAH features in the Spitzer IRS spectrum. The disk model reproduces the observed SED and also the HST image shown below. Lower left panel: HST data; lower right panel: model.

of the radiation field at the location where the photons were absorbed. We include these figures to illustrate our cautionary notes on modeling edge-on disks and also to show the new extensions to our codes for incorporating emission from a population of very small non-equilibrium grains.

5 Disk images

High resolution multiwavelength disk imaging complements spectral data in removing degeneracies in modeling and enabling disk properties such as the outer radius and the spatial variation of dust properties to be determined.

The first HST images of edge-on disks seen in reflected starlight clearly demonstrated that flared disks with dust suspended high above the midplane were a reality with the HST images closely resembling predictions of scattered light models (Whitney & Hartmann 1992). Edge-on disks act as a natural coro-

nagraph with the dense midplane blocking out direct starlight that would otherwise overwhelm the much fainter scattered light from the disk. To date most disks imaged in scattered light are edge-on systems and studying them provides information on disk structure and the scattering properties of the circumstellar dust (Watson et al. 2007). Multiwavelength images (optical through near infrared) of edge-on disks yield information on the wavelength dependence of the circumstellar dust opacity, since the width of the dust lane is wavelength dependent (Wood et al. 1998; Cotera et al. 2001; Watson & Stapelfeldt 2004). Images also reveal the outer radius of the disk, which as mentioned earlier is very hard to determine from modeling disk spectra. Coronagraphs on HST’s NICMOS instrument and ground based adaptive optics systems, together with careful PSF fitting and removal of direct starlight, have enabled non edge-on disks to be imaged in scattered light (Krist et al. 2000).

Disk images at very long wavelengths provide further clues to the size of the circumstellar dust that dominates the long wavelength thermal emission (Beckwith & Sargent 1991; Natta et al. 2007). Spectacular ground based mid infrared adaptive optics imaging is now probing AU sizescales in disks and providing further information on the dust content and chemistry of disks. The promise of very high angular resolution images from ALMA will allow direct imaging of annular gaps predicted to be swept out by disk-planet interactions, again this information is not readily accessible from spectra alone.

6 Disk studies with Spitzer

For the last few years star formation observers, modelers, and theoreticians have been drinking from the Spitzer firehose of spectacular infrared images and high resolution spectra. One of the major contributions from Spitzer is the availability of large datasets allowing us to study disks over a wide range of ages and environments, from young, dense clusters such as the Orion Nebula Cluster to old, low density clusters where the majority of the protostellar disks have been dispersed leaving very tenuous disks exhibiting small infrared excesses.

6.1 *Transition disks*

As mentioned earlier, Spitzer observations have greatly increased the number of disks with infrared deficits indicative of large inner holes and gaps. These observations in turn have spurred on theoretical models for disk evolution and the opening up of gaps in the inner disk regions. Among the popular models for gap opening are disk-planet interactions (Lin & Papaloizou 1979a, b;

Artymowicz & Lubow 1994); photoevaporation of the inner disk by ultraviolet starlight (Alexander et al. 2006); and evacuation of the inner disk by the magneto-rotational instability (Chiang et al. 2007). All of these models must clear the inner disk regions of dust out to tens of AU. Some of the disks observed still exhibit signatures of accretion, implying that gas accretes through the dust free inner regions.

Gaps in disks have long been predicted to arise through disk-planet interactions and recent models for the GM Aur disk (Rice et al. 2003, 2006) suggest that its infrared spectrum may be explained by a planet opening up a gap within the disk. The observable accretion signatures from GM Aur require gas inside the dust disk and the “disk filtration” model of Rice et al. (2006) provides a mechanism where large and small dust grains are filtered with only small grains being dragged through the gap by the accreting gas. This filtration mechanism naturally produces the observed infrared deficits since the dust content of the inner disk is greatly reduced, while still allowing disk material to accrete onto the star. In models of disk-planet interactions the disks may simply be caught at an epoch where a planet has opened up a gap in the disk. If the planet migrates in to the star the gap may close and the disk spectrum would no longer exhibit an infrared deficit. Such disks may not represent an evolutionary sequence implied by the name “transition disk,” instead being transitory phenomena.

On the other hand, models of disk evolution that invoke photoevaporation and clearing by the magneto-rotational instability (e.g., Chiang et al. 2007) do firmly place the transition disks into a distinct evolutionary phase between massive optically thick and more tenuous optically thin disks. Depending on stellar properties and the disk viscosity, these models produce an inside-out evolution of disks whereby the inner disk regions are cleared of dust, but still allowing for gas accretion. At later times, the outer disk may be cleared by photoevaporation. It is likely that some combination of disk-planet interactions, photoevaporation, and magneto-rotational instabilities result in the observed near infrared deficits of transition disks.

6.2 *Disk lifetimes*

Observations of excess emission from disks in many star clusters from near infrared through submillimetre wavelengths have enabled more constraints to be placed on the disk fraction versus age relationships first presented by Haisch et al. (2001). Submillimetre observations (e.g., Carpenter et al. 2005) provide estimates of disk masses versus age, while sensitive Spitzer 70 μm observations extend the detected disk mass range down to very small levels as low as $M_{\text{dust}} \sim 10^{-9} M_{\odot}$ for cluster ages above 10^8 years (see review by

Meyer et al. 2007). Overall there is a large spread of disk masses with age, but with increasing data some trends are emerging suggesting a t^{-1} disk mass evolution transitioning to a more rapid t^{-2} evolution at later times. Models of disk evolution must therefore explain the mass-age spread and also the evolution of disk masses and disk clearing with time.

6.3 Disk structure, dust grain growth, & settling

Spectroscopy from Spitzer's IRS instrument in the $5\mu\text{m}$ to $30\mu\text{m}$ range probes dust settling within disks (D'Alessio et al. 2006), the silicate features (Forrest et al. 2004), and the presence of transiently heated very small grains and PAH molecules (e.g., Pontoppidan et al. 2007). As with earlier studies, a range of disk shapes are inferred from the IRS continuum showing that large dust grains in disks may or may not be coupled to the gas in vertical hydrostatic equilibrium. Disk chemistry, in particular the crystallinity studies, have benefited greatly from the large amounts of IRS spectra showing the varied shapes of mid infrared silicate features. The inclusion in models of emission from transiently heated grains and molecules, especially for disks around massive stars, is required otherwise color-color diagrams and spectral modeling of mid infrared data could result in misclassification of many objects.

6.4 Modeling large datasets

With the very large datasets for hundreds of disk systems in the Spitzer archive it is desirable to have automated tools for fitting spectra and determining disk properties. Several options are available to estimate disk properties from large datasets including using the very fast semi-analytic codes (such as presented by Chiang & Goldreich 1997) and using pre-computed grids of models for circumstellar disks and envelopes (e.g., Robitaille et al. 2006, 2007).

The on-line grid of models and associated fitting tool presented by Robitaille et al. (2006, 2007) fits datasets to give ranges of model parameters for the star and circumstellar material (disks and envelopes), along with estimates for the interstellar extinction to the object. The grid and on-line fitting tool has been tested against data for the Taurus star forming region and does a very good job at reproducing star, disk, and envelope properties in the literature from previous studies of individual sources. By presenting the statistical best fit model along with the range of acceptable fits the user can avoid over-interpreting data. The wider the wavelength coverage available, the tighter the constraints on system properties as demonstrated in Figure 5 for the AA Tau disk. Using this on-line fitting tool with multiwavelength datasets enables the

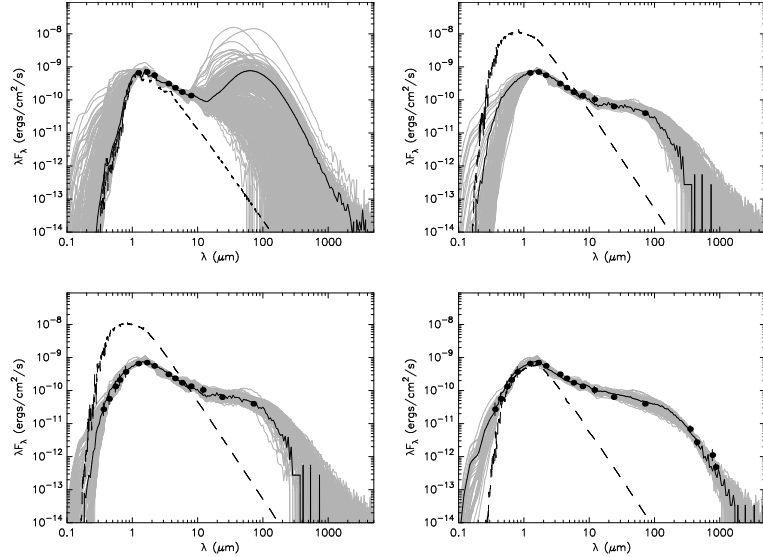


Fig. 5. Data and models for the disk system AA Tau. Notice that the number of models providing good fits decreases as data from a wider wavelength range is included.

user to identify many of the degeneracies in classification inherent in color-color analysis, which typically use data from only four often closely separated wavelengths.

7 Looking to the future

One of the key areas of disk research over the coming years will be the thorough testing of observational signatures of disk evolutionary models including dust growth, chemistry, inside out evolution, and disk-planet interactions. Current and planned large datasets spanning optical through mm wavelengths, high spatial and spectral resolution data, and time variability studies will place tighter constraints on disk models. Disk masses are currently not well constrained and hopefully this can be remedied with careful modeling of dust properties and disk structure. Interferometric imaging of disk gaps and the innermost regions will be especially exciting. Near and mid infrared interferometry is just beginning to return data on inner disk regions and this promises to become a very active area and the data will undoubtedly demand improved theoretical disk models both from a dynamical and radiation transfer perspective.

References

Adams, F., & Shu, F. 1986, *ApJ*, 308, 836

Akeson, R., et al. 2005, *ApJ*, 622, 440
 Alexander, R., Clarke, C., & Pringle, J. 2006, *MNRAS*, 369, 229
 Andre, P., Ward-Thompson, D., & Barsony, M. 2000, *PPIV*, p59
 Artymowicz, P., & Lubow, S. 1994, *ApJ*, 421, 651
 Beckwith, S., & Sargent, A. 1991, *ApJ*, 381, 250
 Beckwith, S., Sargent, A., Chini, R., & Guesten, R. 1990, *AJ*, 99, 924
 Bjorkman, J., & Wood, K. 2001, 554, 615
 Bjorkman, J., Whitney, B., & Wood, K. 2002, *BAAS*, 201, 4901
 Bouvier, J., Alencar, S., Harries, T., Johns-Krull, C., & Romanova, M. 2007, *PPV*, p479
 Calvet, N., et al. 2005, *ApJ*, 630, L185
 Calvet, N., Magris, G., Patino, A., & D'Alessio, P. 1992, *RMxAA*, 24, 27
 Carpenter, J., Wolf, S., Schreyer, K., Launhardt, R., & Henning, T. 2005, *AJ*, 129, 1049
 Chiang, E., & Murray-Clay, R. 2007, *Nature Physics*, 3, 604
 Chiang, E., et al. 2001, *ApJ*, 547, 1077
 Chiang, E., & Goldreich, P. 1999, *ApJ*, 519, 279
 Chiang, E., & Goldreich, P. 1997, *ApJ*, 490, 368
 Cotera, A., et al. 2001, *ApJ*, 556, 958
 D'Alessio, P., Calvet, N., Hartmann, L., Franco-Hernandez, R., & Servin, H. 2006, *ApJ*, 638, 314
 D'Alessio, P., Merin, B., Calvet, N., Hartmann, L., & Montesinos, B. 2005, *RMxAA*, 41, 61
 D'Alessio, P., Calvet, N., & Hartmann, L. 2001, *ApJ*, 553, 321
 D'Alessio, P., Calvet, N., Hartmann, L., Lizano, S., & Canto, J. 1999, *ApJ*, 527, 893
 D'Alessio, P., Canto, N., Calvet, N., & Lizano, S. 1998, *ApJ*, 500, 411
 Draine, B., & Lee, H. *ApJ*, 285, 89
 Draine, B., & Li, A. 2007, *ApJ*, 657, 810
 Dullemond, C.P., et al. 2007, *A&A*, 473, 457
 Dullemond, C.P., Hollenbach, D., Kamp, I., & D'Alessio, P. 2007, *PPV*, p555
 Dullemond, C.P., & Dominik, C. 2005, *A&A*, 434, 971
 Dullemond, C.P., & Dominik, C. 2004, *A&A*, 417, 159
 Dullemond, C.P., Dominik, C., & Natta, A. 2001, *ApJ*, 560, 957
 Espaillat, C., et al. 2007, *ApJ*, 664, 111
 Forrest, W., et al. 2004, *ApJS*, 154, 443
 Furlan, E., et al. 2007, *ApJ*, 664, 1176
 Habart, E., Natta, A., Testi, L., & Carbillet, M. 2006, *A&A*, 449, 1067
 Haisch, K., Lada, E., & Lada, C. 2001, *ApJ*, 553, 153
 Hartmann, L., Kenyon, S., & Calvet, N. 1993, *ApJ*, 407, 219
 Hillenbrand, L., Strom, S., Vrba, F., Keene, J. 1992, *ApJ*, 397, 613
 Indebetouw, R., Whitney, B., Johnson, K., & Wood, K. 2006, *ApJ*, 636, 362
 Isella, A., & Natta, A. 2005, *A&A*, 438, 899
 Kamp, I., & Dullemond, C. 2004, *ApJ*, 615, 991
 Kenyon, S., et al. 1994, *AJ*, 107, 2153

Kenyon, S., & Hartmann, L. 1987, *ApJ*, 323, 714
 Koerner, D., Sargent, A., & Beckwith, S. 1993, *Icarus*, 106, 2
 Krist, J., et al. 2000, *ApJ*, 538, 793
 Lada, C., et al. 2006, *AJ*, 131, 1574
 Lada, C., & Adams, F. 1992, *ApJ*, 393, 278
 Lada, C. 1987, in *IAU Symp. 115: Star Forming Regions*, ed. M. Peimbert & J. Jugaku, p1
 Lin, D., & Papaloizou, J. 1979, *MNRAS*, 188, 191
 Lin, D., & Papaloizou, J. 1979, *MNRAS*, 186, 799
 Lucy, L. 1999, *A&A*, 344, 282
 Lynden-Bell, D., & Pringle, J. 1974, *MNRAS*, 168, 603
 Mathis, J., Rumpl, W., & Nordsieck, K. 1977, *ApJ*, 217, 425
 Meeus, G. et al. 2001, *A&A*, 365, 476
 Mendoza, E.E. 1968, *ApJ*, 151, 977
 Meyer, M., Backman, D., Weinberger, A., & Wyatt, M. 2007, *PPV*, p573
 Miyake, K., & Nakagawa, Y. 1995, *ApJ*, 441, 361
 Najita, J., Carr, J., Glassgold, A., & Valenti, J. 2007, *PPV*, p507
 Natta, A., et al. 2007, *PPV*, p767
 Natta, A., et al. 2001. *A&A*, 371, 186
 Nomura, H., AiKawa, Y., Tsujimoto, M., Nakagawa, Y., & Millar, T. 2007, *ApJ*, 661, 334
 Pringle, J. 1981, *ARA&A*, 19, 137
 Pontoppidan, K., et al. 2007, *ApJ*, 656, 980
 Rice, W., Armitage, P., Wood, K., & Lodato, G. 2006, *MNRAS*, 373, 1619
 Rice, W., Wood, K., Armitage, P., Whitney, B., & Bjorkman, J. 2003, *MNRAS*, 342, 79
 Robitaille, T., Whitney, B., Indebetouw, R., & Wood, K. 2007, *ApJS*, 169, 328
 Robitaille, T., Whitney, B., Indebetouw, R., Wood, K., & Denzmore, P. 2006, *ApJS*, 167, 256
 Ruiz, M., et al. 1987, *ApJ*, 316, L21
 Scholz, A., Jayawardhana, R., & Wood, K. 2006, *ApJ*, 645, 1489
 Shakura, N., & Syunyaev, R. 1973, *A&A*, 24, 337
 Tannirkulam, A., Harries, T., & Monnier, J. 2007, *ApJ*, 661, 374
 Varniere, P., et al. 2006, *ApJ*, 637, L125
 Vink, J., Harries, T., & Drew, J. 2005, *A&A*, 430, 213
 Watson, A., Stapelfeldt, K., Wood, K., & Menard, F. 2007, *PPV*, p523
 Watson, A., & Stapelfeldt, K. 2004, *ApJ*, 602, 860
 Whitney, B., Wood, K., Bjorkman, J., & Wolff, M. 2003, *ApJ*, 591, 1049
 Whitney, B., & Hartmann, L. 1992, *ApJ*, 395, 529
 Wolf, S. 2003, *Comp. Phys. Comm.* 15, 99
 Wolf, S., Gueth, F., Henning, T., & Kley, W. 2002, *ApJ*, 566, L97
 Wood, K., Kenyon, S., Whitney, B., & Turnbull, M. 1998, *ApJ*, 497, 404
 Wood, K., Bjorkman, K., & Bjorkman, J. 1997, *ApJ*, 477, 926